How the Intracluster Medium Affects the Far-Infrared–Radio Correlation within Virgo Cluster Galaxies

E.J. Murphy,[1,2] J.D.P. Kenney,[1] G. Helou,[3] A. Chung,[4] and J.H. Howell[2]

ABSTRACT

We present a study on the effects of the intracluster medium (ICM) on the interstellar medium (ISM) of 10 Virgo cluster galaxies using *Spitzer* far-infrared (FIR) and VLA radio continuum imaging. Relying on the FIR-radio correlation *within* normal galaxies, we use our infrared data to create model radio maps which we compare to the observed radio images. For 6 of our sample galaxies we find regions along their outer edges that are highly deficient in the radio compared with our models. We believe these observations are the signatures of ICM ram pressure. For NGC 4522 we find the radio deficit region to lie just exterior to a region of high radio polarization and flat radio spectral index, however the total radio continuum in this region does not appear significantly enhanced. This scenario seems consistent for other galaxies with radio polarization data in the literature. We also find that galaxies having local radio deficits appear to have enhanced global radio fluxes. Our preferred physical picture is that the observed radio deficit regions arise from the ICM wind sweeping away cosmic-ray (CR) electrons and the associated magnetic field, thereby creating synchrotron tails observed for some of our galaxies. CR particles are also re-accelerated by ICM-driven shocklets behind the observed radio deficit regions which in turn enhances the remaining radio disk brightness. The high radio polarization and lack of coincidental signatures in the total synchrotron power in these regions arises from shear, and possibly mild compression, as the ICM wind drags and stretches the magnetic field.

Subject headings: clusters: general — infrared: galaxies — radio continuum: galaxies — cosmic-rays — galaxies: interactions — galaxies: ISM

1. Introduction

The physical processes associated with interactions between the intracluster medium (ICM) and the interstellar medium (ISM) play critical roles driving the evolution of spiral galaxies in clusters (e.g. Gunn & Gott 1972; Larson, Tinsley, & Caldwell 1980; Abadi, Moore, & Bower 1999; Schulz & Struck 2001; Vollmer et al. 2001). Galaxies are preferentially found in groups or clusters where most of these processes occur, yet many basic effects related to ICM-ISM interactions (i.e. ram pressure stripping) are still not well understood. These effects include the fate of star-forming molecular clouds, the rates of triggered star

[1]Department of Astronomy, Yale University, P.O. Box 208101, New Haven, CT 06520-8101

[2]*Spitzer* Science Center, MC 314-6, California Institute of Technology, Pasadena, CA 91125; emurphy@ipac.caltech.edu

[3]California Institute of Technology, MC 314-6, Pasadena, CA 91125

[4]Jansky Fellow of the NRAO at the University of Massachusetts, Amherst, MA 01003

formation versus gas removal, and the possible reconfiguration of a galaxy's large-scale magnetic field and/or cosmic-ray (CR) particles.

Since ram pressure will more easily affect lower density constituents of the ISM, it seems that the diffuse radio continuum halos of galaxies may be sensitive tracers of active ICM pressure as indicated by observations for a number of Virgo cluster spirals including NGC 4522 (Vollmer et al. 2004), NGC 4402 (Crowl et al. 2005), NGC 4254 (Chyży, Ehle, & Beck 2007), and a few others (Vollmer et al. 2007; Chung et al. 2007). More specifically, large regions of enhanced polarized radio continuum emission have been found within a number of cluster spirals (Vollmer et al. 2007; Chyży, Ehle, & Beck 2007); the maxima of the polarized radio continuum distributions within these galaxies are located along outer edges and thought to arise from external influences of the cluster environment. However, without a good idea of the galaxy's unperturbed appearance in the radio, these observations alone make it difficult to quantify the extent of ram pressure effects. We now address this comparison using the nearly universal correlation between the far-infrared (FIR) and non-thermal radio continuum emission of normal galaxies (e.g. de Jong et al. 1985; Helou, Soifer, & Rowan-Robinson 1985).

Using a phenomenological smearing model, in which a galaxy's FIR map is smoothed by a parameterized kernel to compensate for the fact that the mean free path of dust heating photons is much shorter than the diffusion length of CR electron, Murphy et al. (2008a) has shown for a sample of 15 non-Virgo spiral galaxies that the dispersion in the FIR/radio ratios on sub-kiloparsec scales *within* galaxies can be reduced by a factor of $\sim$2, on average. Accordingly, it is possible to obtain a good first order approximation of an undisturbed galaxy's non-thermal radio continuum morphology with its FIR image alone.

Coupling FIR observations taken by the *Spitzer* Space Telescope with VLA radio continuum imaging, obtained as part of the VLA Imaging of Virgo in Atomic gas (VIVA; A. Chung et al. 2008, in preparation) survey, we study how the relativistic and gaseous phases of the ISM are affected by ICM-ISM interactions for a sample of Virgo cluster galaxies. This is done using FIR *Spitzer* maps to predict how the radio morphology should appear if the galaxy resided in the field; in this paper we make the case that significant deviations from such an appearance are directly related to ICM-ISM interactions. See Murphy et al. (2008b) for the complete study.

2. Observations and Analysis

A total of $\sim$40 of the 53 VIVA sample galaxies are included in the *Spitzer* Survey of Virgo (SPITSOV; see J.D.P. Kenney et al. 2008, in preparation; J.D.P Kenney et al. this proceedings) imaging program. At the time of this writing, a sub-sample of 10 galaxies had existing high quality FIR and radio continuum maps. *Spitzer* imaging was carried out for each galaxy using the Multiband Imaging Photometer for *Spitzer* (MIPS; Rieke, et al. 2004). The strategy of the imaging campaign was based on that of the Spitzer Infrared Nearby Galaxies Survey (SINGS; Kennicutt et al. 2003) with the only difference being a factor of 2 increase in exposure times to better detect diffuse emission arising in the outer regions of the Virgo sample galaxies.

The 1.4 GHz radio continuum maps were created from the line-free channels of H I data cubes collected as part of of the VIVA survey; a detailed description of the VLA observations along with the H I reductions and associated data products can be found in A. Chung et al. (2008, in preparation). To perform accurate comparative analysis between the MIPS and radio data we match the resolution of the final calibrated images using the MIPS PSF. After cropping each set of galaxy images to a common field of view we CLEANed the radio data and convolved the resulting CLEAN components with a model of the MIPS 70 μm PSF.

2.1. Modeled Radio Continuum Maps

Detailed studies of the FIR-radio correlation within nearby field galaxies (e.g. Murphy et al. 2006a, 2008a) have shown that the dispersion in the FIR/radio ratios on $\gtrsim 0.1 - 1$ kpc scales within galaxy disks is similar to the dispersion in the global FIR-radio correlation (i.e. $\lesssim 0.3$ dex). This strong correlation between the FIR and radio images of spirals has been found to improve by a factor of ~ 2 using an image-smearing technique which approximates a galaxy radio image as a smoother version of its FIR image due to the diffusion of CR electrons. While the star-forming disks of cluster galaxies are often truncated due to the gas stripping events, the 70 μm images for the entire sample do not appear to be more strongly disturbed than galaxies in the field; we do not observe sharp edges, tails, or clear evidence for extraplanar emission at 70 μm. Therefore, we apply the image-smearing technique of Murphy et al. (2006b, 2008a) (using a single smoothing function) to create models for the expected radio distribution of a galaxy assuming that the FIR/radio ratio map is like that of a field galaxy.

NGC 4330   NGC 4402   NGC 4522

Fig. 1.— The radio deficit regions of NGC 4330, NGC 4402, and NGC 4522 with radio continuum contours. The radio continuum contours begin at the 3-σ RMS level and increase logarithmically. For each galaxy we find the deficit region to be located on the edge opposite that of the observed synchrotron tails.

2.2. Deviations from Expectations for Field Galaxies

Our aim is to determine if differences between the observed and modeled radio continuum images arise from ICM-ISM interactions and, if so, whether quantifying and comparing such differences within our sample can help improve our current physical picture of such interactions. We therefore create ratio maps between the observed and modeled radio maps in the following manner. We divide the observed radio map by the modeled radio map after having removed pixels not detected at the 5-σ RMS level of the modeled map only. Pixel values in the ratio map ≥ 1.3 and ≤ 0.5 are considered to be excesses and deficits, respectively; for a more complete description on how radio deficit and excess regions were determined see Murphy et al. (2008b).

For most (60%) of our sample galaxies we detect radio deficit regions which are located along a single edge of their disks and opposite of any identified H I tails. The radio deficit regions are also generally found to be opposite any radio excess regions associated with synchrotron tails; this is illustrated in Figure 1 for NGC 4330, NGC 4402, and NGC 4522. Since these H I and synchrotron tails are likely identifying the direction of the ICM wind, we focus our attention toward the radio deficit regions as they are probing directly the most intense effects of the ongoing ICM-ISM interactions. The combination of these observations suggests that the radio deficit regions likely arise from the same gravitational or gas dynamical effects which

have displaced the galaxy's H I gas and relativistic plasma. We therefore believe that the radio deficit regions identify the zone in which the ICM wind is actively working on each galaxy's ISM.

To compare quantitatively the radio deficiencies among the sample galaxies we define the parameter

$$\Upsilon = \frac{(S_\nu^{\mathrm{mod}} - S_\nu^{\mathrm{obs}})_{\mathrm{def}}}{S_\nu^{\mathrm{glob}}} \tag{1}$$

which measures the difference between the observed and modeled radio flux densities within the radio deficit region normalized by the global radio flux density of the galaxy.
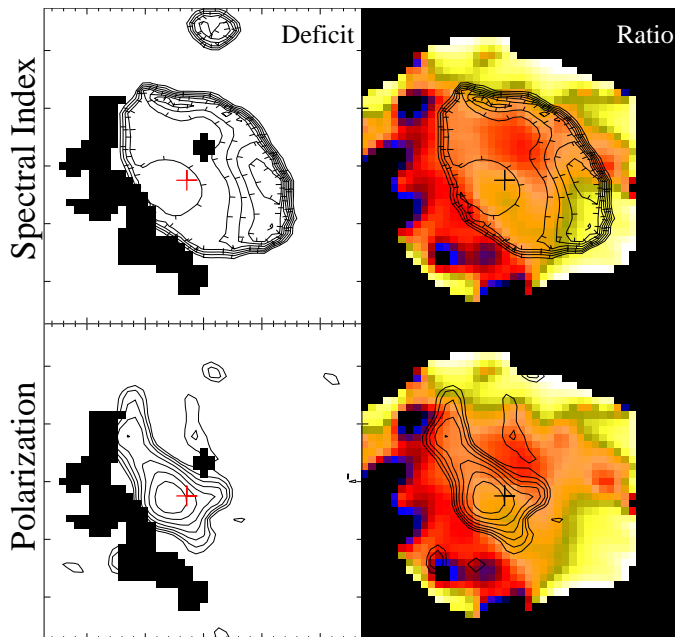

Fig. 2.— In the top panels, from left to right, we plot the radio continuum deficit map and the ratio map of the observed to modeled radio continuum emission of NGC 4522 overlayed with radio spectral index contours taken from Vollmer et al. (2004). The contour levels increase by 0.2 and range between −1.9 to −0.3; the dashes indicate the direction of the downward gradient. The ratio maps is show in a logarithmic stretch ranging from 10% (dark) to a factor of 3 (light). We plot the same images in the bottom panels except this time we overlay them with polarized radio contours (Vollmer et al. 2004). The contours are logarithmically scaled and begin at the 3-σ RMS level. The cross in each panel identifies the center of the galaxy.

3. NGC 4522: Comparison of Radio Deficit Region with Radio Polarization and Spectral Index Maps

Radio polarization and spectral index data of NGC 4522 provide evidence for an ongoing ICM-ISM interaction (Vollmer et al. 2004); the eastern edge of NGC 4522 is found to be highly polarized and coincident with the flattest spectral index which steepens towards the western side of the galaxy. In the first column of Figure 2 we plot the radio continuum deficit regions and overlay the 20 to 6 cm spectral index and 6 cm polarized radio continuum maps of (Vollmer et al. 2004). We find that the regions of high polarization and flattest spectral index lie just interior to the radio deficit region. While the peak in the polarized radio continuum is coincident with the flattest part of the spectral index distribution, this is not where the total radio intensity (or FIR) peaks as pointed out by (Vollmer et al. 2004).

These observations suggest that any pre-existing gradient in the observed FIR/radio ratio distribution will be stronger than deviations arising from the effects of ram pressure and that, to first order, star formation in the disk drives the appearance of the FIR/radio ratios. However, by inspecting the ratio map of NGC 4522 displayed in the second column of Figure 2, which was created using our *smoothed* 70 μm image, ICM-ISM effects become more apparent. We find slightly higher ratios (i.e. ratios of $\sim$90%) near the regions of high radio polarization and flat spectral indices; the elevated ratios in these regions are therefore attributed to a modest increase in the total radio continuum. We now try to determine the most plausible physical scenario to explain this combination of observations.

4.   Discussion

We have shown that a large fraction of our sample of cluster galaxies exhibits statistically significant radio deficit regions relative to what the phenomenological image-smearing model of Murphy et al. (2008a) would predict within their disks. Such deficit regions are not found within normal field galaxies suggesting that cluster environment processes are likely at work. Comparing our results with other observational data for NGC 4522, a galaxy which is clearly experiencing the effects of ram pressure, we find our deficit region agrees with such a scenario and may be able to add new insight on the magnitude of the interaction.

Similar to the example of NGC 4522, radio polarization observations of other Virgo cluster galaxies exhibit highly polarized radio emission along the predicted leading edges between their ISM and the ICM wind (Vollmer et al. 2007; Chyży, Ehle, & Beck 2007). For the galaxies overlapping in our sample which show evidence for being disturbed (i.e. NGC 4254, NGC 4388 and NGC 4402), the regions of highly polarized continuum emission are coincident with local radio continuum enhancements found in our ratio maps (i.e. ratios of $\sim$1.1 $-$ 1.7) and interior to our radio deficit regions. Thus, the scenario described for NGC 4522 seems to be applicable for these galaxies as well based on the polarized radio continuum results. With this picture we will use the findings from our analysis to quantitatively assess the strength of the ram pressure from the intracluster medium (ICM).

4.1.   Estimates of Minimum Ram Pressure and Internal Relativistic ISM Pressure

Ram pressure from the ICM is simply defined as,

$$P_{\mathrm{ram}} = \rho_{\mathrm{ICM}} v_{\mathrm{gal}}^2 \tag{2}$$

where ρ_{ICM} is the ICM mass density and v_{gal} is velocity of a galaxy relative to the ICM. If the ICM ram pressure exceeds that of a galaxy's relativistic ISM (CRs + magnetic field) then it should be possible to redistribute and even strip them from the galaxy disk. Using the predicted radio flux density for each deficit region, we can approximate a minimum value for the ICM ram pressure needed to cause the observed depression in the radio.

Taking the predicted flux density of the deficit region along with its area we use the revised equipartition and minimum energy formulas of Beck & Krause (2005) to calculate the minimum energy magnetic field strength of the deficit regions. This calculation assumes a proton-to-electron number density ratio of 100, a radio spectral index of -0.85, and a path length through the emitting medium of $1/cos(i)$ kpc where i is the galaxy inclination. Using these magnetic field strengths B (i.e. calculated using Equation 4 of Beck & Krause (2005)) we compute the magnetic field energy densities $U_{\mathrm{B}} = B^2/(8\pi)$ of the deficit regions.

Assuming minimum energy between the magnetic field and CR particle energy densities, U_B and U_{CR} respectively, we can use the values of U_B over the deficit region in our model to determine the minimum P_{ram} necessary to create the deficit regions. From minimum energy arguments we find that $U_B = 3/4 U_{CR}$. For a relativistic gas the magnetic pressure, P_B, and CR pressure P_{CR} are related to energy density such that $P_B = U_B$ and $P_{CR} = 1/3 U_{CR}$ leading to the relation that $P_{CR} = 4/9 U_B$. Then, the pressure of the relativistic ISM is found to be

$$P_{RISM} = P_{CR} + P_B \sim 13/9 U_B. \tag{3}$$

These estimates, denoted as P_{RISM}^{mod} set the minimum ICM ram pressure necessary to create the observed radio continuum deficit regions (i.e. $P_{ram} > P_{RISM}^{mod}$).

All galaxies have P_{RISM}^{mod} values between $\sim 2 - 4 \times 10^{-12}$ dyn cm^{-2}. Using the projected linear distances to the cluster center among our sample along with a measured density profile of Virgo (Matsumoto et al. 2000) yields a range in ICM density of $n_{ICM} = \rho_{ICM}/m_p \approx 0.6 - 4 \times 10^{-4}$ cm^{-3}. Taking a typical Virgo galaxy velocity of 1500 km s^{-1} (Kenney, van Gorkom, & Vollmer 2004) the associated range in ICM ram pressure is $P_{ram} \approx 2 - 15 \times 10^{-12}$ dyn cm^{-2}. This range of ICM pressures is generally greater or similar to the values for P_{RISM}^{mod} which is consistent with ICM ram pressure being able to create the observed deficit regions. We also note that these pressures agree with those produced in the 3D hydrodynamical simulation of Roediger & Brüggen (2007) over the same projected linear distances to the cluster center among our sample.
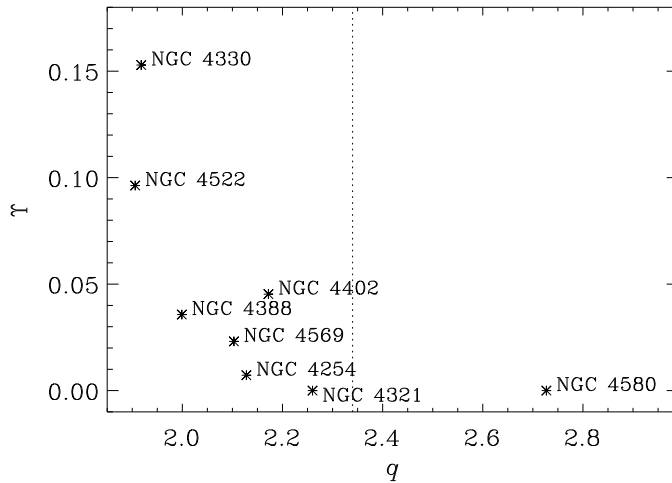

Fig. 3.— The severity of the deficit region characterized by Υ plotted against q (the logarithmic FIR/radio ratio). The vertical line at $q = 2.34$ identifies the average q value reported by Yun, Reddy, & Condon (2001) for 1809 galaxies.

4.2. Cosmic Ray Electron Escape and Re-acceleration

While the CR electrons are being moved around by the ICM wind, it does not appear that they escape the galaxy disks as global q (logarithmic FIR/radio) ratios do not appear systematically high with respect to the nominal value of $\sim 2.34 \pm 0.26$ dex (i.e. Yun, Reddy, & Condon 2001). In fact, by plotting q against Υ (our parameter defining the severity of the deficit region) in Figure 3 we find a trend of decreasing FIR/radio ratio with increasing Υ and that nearly all of the q values are lower than the nominal value. Other, more detailed studies on the global FIR and radio properties of cluster galaxies, have pointed out notably lower

FIR/radio ratios than expected from the FIR-radio relation in the field (Miller & Owen 2001; Reddy & Yun 2004). This suggests that there is either depressed FIR emission or an enhancement in the global radio emission among our sample galaxies. And while the trend in Figure 3 may simply be the result of small number statistics, it also might be suggestive that q itself is sensitive to the strength of the ICM ram pressure and perhaps a galaxy's stripping history.

The only major exception in our sample is NGC 4580 which has a very high q value; this galaxy also has the highest H I deficiency among the sample (a factor of 5 larger than the median). It is also thought to have been stripped long ($\sim$400 Myr) ago and is the only post-strongly stripped galaxy observed so long after peak pressure (Crowl & Kenney 2008). We therefore speculate that its high q value is the result of CR electron escape as the ICM wind has swept out most of the galaxy's gaseous and relativistic ISM long ago.

While it is still not completely clear, we believe the most plausible explanation for the depressed q values seems to be that of the ICM wind raising the global CR electron energy and synchrotron power by driving shocklets into the ISM which are re-accelerating CR electrons. The fact that we only find moderate local enhancements to the total continuum behind the radio deficit region suggests that the shocks run through the entire galaxy disk rather quickly. The shock speed, v_{s}, which must be super-Alfvénic to re-accelerate CR electrons, should have a value around

$$v_{\mathrm{s}} \approx \left(\frac{4}{3}\frac{P_{\mathrm{ram}}}{\rho_{\mathrm{ISM}}}\right)^{1/2} \approx v_{\mathrm{gal}}\left(\frac{4}{3}\frac{\rho_{\mathrm{ICM}}}{\rho_{\mathrm{ISM}}}\right)^{1/2}, \tag{4}$$

where P_{ram} is the ram pressure, as defined in Equation 2, and ρ_{ISM} and ρ_{ICM} are the ISM and ICM densities, respectively. Taking $v_{\mathrm{gal}} \approx 1500$ km s^{-1}, $n_{\mathrm{ISM}} = \rho_{\mathrm{ISM}}/m_p \approx 1$ cm^{-3}, and the range in ρ_{ICM} values discussed leads to shock velocities ranging between $\sim$10 to 35 km/s. Assuming a thin disk thickness of 500 pc, the shocks should run through each disk on the order of $\sim$15 to 50 Myr; indeed this is very short compared to the dynamical timescale of these systems.

5. Summary and Conclusions

We have studied the interstellar medium (ISM) of 10 Virgo galaxies included in the VLA Imaging of Virgo in Atomic Gas (VIVA) survey using *Spitzer* MIPS and VLA 20 cm imagery. By comparing the observed radio continuum images with modeled distributions, created using a phenomenological image-smearing model described by Murphy et al. (2006b, 2008a), we find that the edges of many cluster galaxy disks are significantly radio deficient. These radio deficit regions are consistent with being areas affected by intracluster medium (ICM) induced ram pressure as suggested by the location of H I and radio continuum tails. From our results we are able to conclude the following:

1. The distribution of radio/FIR ratios within cluster galaxies thought to be experiencing ICM-ISM effects are systematically different from the distribution in field galaxies; radio/FIR ratios are found to be significantly low along galaxy edges probably in the direction of the ICM wind arising from a local deficit of radio continuum emission.

2. In the case of NGC 4522 we find that the radio deficit region lies exterior to a region of high radio polarization and a flat radio spectral index. We interpret this to suggest that CR electrons in the halos of galaxies are being swept up by the ICM wind. The ICM wind drives shocklets into the ISM of the galaxy which re-accelerate CR particles interior to the working surface at the ICM-ISM interface.

Some CR electrons may also be redistributed downstream creating synchrotron tails as observed for NGC 4522. The high radio polarization is probably the result of shear as the ICM wind stretches the magnetic field; compression may also play a role, though a modest one, since the total radio continuum in these regions does not appear significantly enhanced.

3. The global radio/FIR ratios of these cluster galaxies are systematically higher than the average value found for field galaxies and appear to increase with increasing severity of the ISM stripping. We attribute this to a greater relative increase in the CR energy density pursuant to a more sever effect of stripping on the galaxy.

4. Using the identified radio deficit regions we are able to get a quantitative estimate of the minimum strength of the ICM pressure required to affect a galaxy disk; we find values in the range of $\sim 2 - 4 \times 10^{-12}$ dyn cm^{-2}. These pressures are generally smaller than, but similar to, those estimated for typical values of the ICM gas density and galaxy velocities, as well as the range of ram pressures calculated by 3D hydrodynamical simulations; therefore, our estimates are consistent with scenario of ram pressure creating the observed deficit regions.

REFERENCES

Abadi, M. G., Moore, B., and Bower, R. G. 1999, MNRAS308, 947

Beck, R. and Krause, M. 2005, Astronomische Nachrichten, 326, 414

Chung, A., van Gorkom, J. H., Kenney, J. D. P., and Vollmer, B. 2007, ApJ, 659, L115

Chyży, K. T., Ehle, M., and Beck, R. 2007, A&A, 474, 415

Crowl H.H., Kenney J.D.P., van Gorkom J.H., and Vollmer B., 2005, AJ, 130, 651

Crowl, H.H. and Kenney, J. D. P. 2008, ApJ, submitted

de Jong, T., Klein, U., Wielebinski, R., and Wunderlich, E. 1985, A&A, 147, L6

Gunn, J. E. and Gott, J. R. I. 1972, ApJ, 176, 1

Helou, G., Soifer, B. T., and Rowan-Robinson, M. 1985, ApJ, 298, L7

Kenney, J.D.P., van Gorkom, J.H., and Vollmer, B. 2004, AJ, 127, 3361

Kennicutt, R. C. Jr., et al. 2003, PASP, 115, 928

Larson, R. B., Tinsley, B. M., and Caldwell, C. N. 1980, ApJ, 237, 692

Matsumoto H., Tsuru T. G., Fukazawa Y., Hattori M. and Davis D. S., 2000, PASJ, 52, 153

Miller, N. A. and Owen, F. N. 2001, AJ, 121, 1903

Murphy E. J., et al. 2006a, ApJ, 638, 157

Murphy E. J., et al. 2006b, ApJ, 651, L111

Murphy E. J., Helou, G., Kenney, J. D. P., Armus, L, and Braun, R. 2008, ApJ, 679, in press (arXiv:0801.4768)

Murphy E. J., Kenney, J. D. P., Helou, G., Chung, A., and Howell, J.H., 2008, ApJ, submitted

Reddy, N. A. and Yun, M. S. 2004, ApJ, 600, 695

Rieke, G. H., et al. 2004, ApJS, 154, 25 ApJ, 493, 121

Roediger, E. and Brüggen, M. 2007, MNRAS, in press, (arXiv:0707.2698)

Schulz, S. and Struck, C. 2001, MNRAS, 328, 185

Vollmer, B., Cayatte, V., Balkowski, C., and Duschl, W. J. 2001, ApJ, 561, 708

Vollmer, B., Beck, R., Kenney, J. P. D., and van Gorkom, J. H. 2004, AJ, 127, 3375

Vollmer, B., Soida, M., Beck, R., Urbanik, M., Chyży, K. T., Otmianowska-Mazur, K., Kenney, J. D. P., and van Gorkom, J. H., 2007, A&A, 464, L37

Yun, M. S., Reddy, N. A., and Condon, J. J. 2001, ApJ, 554, 803